Analysis of Powerplant-Airframe Interactions and Study of the Aircraft Energy Needs

Adrian Rubio Cubas*

DAEP, ISAE-SUPAERO, Toulouse, France

ETSIAE, Universidad Politecnica de Madrid (UPM), Madrid, Spain

Xavier Carbonneau, Aleksandar Joksimovic†

Departement of Aerodynamics and Propulsion, ISAE-SUPAERO,

Universite de Toulouse, 31550 TOULOUSE Cedex 4, Toulouse, France

In recent years, tendencies have been emerging to evolve airplanes from the traditional "tube and wing" paradigm to more integrated and efficient platforms. Taking this upcoming trend as a starting point, with Boeing 737 aircraft as the case study platform, the presented work covers two global areas of research: an aerodynamic analysis of powerplant installation and a study of airplane non-propulsive energies. An application case was developed in aircraft preliminary design software *Pacelab*, in order to perform analysis at the aircraft level. Firstly, a detailed insight into promising new propulsive architectures to explore is provided, and a potential for use of over-the-wing nacelle configurations, which have not been largely exploited in civilian airplanes so far, is discussed. The software is upgraded in order to enable introduction of these alternative powerplant configurations as well as the resulting aerodynamic interactions. Secondly, an analysis of the energy breakdown under several operating conditions is carried out in order to quantify the non-propulsive power of the aircraft, as well as to analyse impact of important failure modes on the airplane energy balance. Conclusions are drawn on comprehensive energy managment analysis of a civilian airplane at a preliminary design level.

List of Abbreviations

AC Alternating Current
ACM Air Cycle Machine
APD Aircraft Preliminary Design
APU Auxiliary Power Unit
ATA Air Transport Association
CFD Computational Fluid Dynamics
CPC Cabin Pressure Controllers
DC Direct Current
ECS Environmental Control System
EDP Engine-Driven Pump
EFB Electronic Flight Bag
EMDP Electric Motor-Driven Pump
EO Engineering Object
EWB Engineering Workbench
FAA Federal Aviation Administration
FCOM Flight Crew Operating Manual
FO Functional Object
GPU Ground Power Unit
KD Knowledge Designer
LGTU Landing Gear Transfer Unit
OWN Over-the-wing nacelle configurations
PCU Power Control Unit
PTU Power Transfer Unit
SF Smart Formula
TR Transformer Rectifier
UWN Under-the-wing nacelle configurations
WB Wing-Body

*MSc Aeronautical Engineering (UPM), Ingenieur SUPAERO (ISAE)
†Professor, research engineer at DAEP, ISAE-Supaero

I. Introduction and Objectives

This work is part of the broad contemporary research motivated by the growth of the civil aerospace market as well as environmental and economical constraints imposed on the industry. This global research aims at identifying aircraft architectures beyond the traditional "tube and wing" configuration, in order to reduce fuel consumption, polluting emissions and noise footprint[2] while remaining compliant with the aerospace sector requirements. A promising path to take to achieve these objectives is by developing aeroplanes with highly integrated powerplants. Since the propulsive group in such configurations will play a decisive role in the overall design, this work defines two ways that impact the energy balance of the powerplant. The first one focuses on external aerodynamic interactions between the powerplant and the airframe, whereas the second one looks at the internal energy impact, such as the non-propulsive power extraction from the engine, in form of mechanical power or bleed air offtake. Before this can be accomplished, many specifications must be studied to assess the impact of the new potential architecture, for instance, what the aerodynamics would be like, the systems architecture and the energy production. In order to investigate the aforementioned energy interactions, the work is applied to a specific airplane, the Boeing 737. The reasons for selecting this platform as relevant for this work will be outlined at the end of this chapter.

The first steps of the work consisted of an in-depth bibliographic research. The goal was to determine the aerodynamic influences of two nacelle configurations: under-the-wing nacelle configuration (UWN) and over-the-wing nacelle configuration (OWN). The objective is to gain a more complete view of the possible aerodynamic interactions between the airframe and the podded turbofan engines of a "tube and wing" airplane.

Certain modifications have been performed in Pacelab, which is the preliminary aircraft design software used, introduced later. On the one hand, this is to enable the introduction of a new aircraft configuration, the over-the-wing nacelle one, and on the other hand, to take into account the aerodynamic interferences of the nacelle installation with respect to the rest of the aircraft. An existing model in Pacelab is enhanced so as to adapt it to the real systems architecture by taking into consideration the environmental control, hydraulic, electrical, and ice and rain protection systems.

The objective is to assess the energy balance so that the energy consumed by the engines in terms of drag is reduced, increasing in this way the energy balance, that is, maximising the useful energy. Then, several cases are analysed to determine energy production, its distribution and consumption.

I.A. Framework

The sponsorship chair AEGIS, a collaboration between ISAE-SUPAERO and the group Safran, under which this work has been performed, aims to identify and consolidate the innovative concepts dealing with propulsive architectures that will power the next generations of aircraft. The objective is to create a core of expertise in the domain of innovative propulsive architectures. One of the key aspects of AEGIS is based on the introduction of a propulsive system highly integrated into the aircraft. Therefore, the research will be focused on the aerodynamic impacts and engine bleed associated with these kind of configurations.

I.B. Objectives

First research-based objective is the analysis of the aerodynamic impact in terms of the installation drag of the engines on the aircraft. Eventually, this objective aims to address the installation of new powerplant architectures highly integrated into the aircraft, according to AEGIS goals. The drag contributions of the powerplant are assessed, as well as the interferences with other components of the aircraft. Several ways of installing the powerplant are compared. The software used will be modified so that the results found are visible in the user interface and allow analysing their consequences.

The second research-based objective is the modelling of the aircraft systems, understanding the way they work and the components of which they are composed. It has been carried out using a preliminary model built in *Pacelab SysArc*, software that includes a representation of the environmental control system (ECS), the hydraulics system and the electrical system.

Taking this preliminary modelling as a basis, it has been studied so as to improve it, and consolidate it by adding missing components and connections, as will be detailed later on. Energy requirements are studied, adding losses to the connections and representing several flight conditions and failure modes so as to analyse how the aircraft needs may vary.

I.B.1. Pacelab

Methodology objectives have been set regarding *Pacelab*, the software that has been used for the two aforementioned purposes: systems modelling and the aerodynamic impact analysis. Major areas of its application are preliminary aircraft and systems architecture design, aircraft and cabin configuration, aircraft economics and route analysis and electronic flight bag (EFB)-based flight profile optimisation. In the scope of the study, two of its programmes have been used: *Pacelab APD* and *Pacelab SysArc*, where software modifications can be introduced using the C# programming language.

Pacelab APD performs the modelling, sizing, analysis and optimisation of tube-and-wing aircraft architectures in the conceptual and preliminary design phases. This tool allows the selection from different aircraft models available in a library that are used as a basis from which the user can change the configuration and architecture of the aeroplane, through the definition of the wing, engines, tail surfaces, landing gear, etc. A *Pacelab APD* model is composed of several categories that include the different components, assemblies and sub-assemblies of the aircraft. They are defined by multiple parameters that can be fixed in order to analyse the impact on the configuration. Moreover, the selection of the parameters which are considered as inputs and those which are considered as outputs depending on the analysis to be accomplished. The software will warn the user in case the model is not well constrained. In addition, mission performance analysis can be carried out to assess the aircraft response under different flight conditions.

Pacelab SysArc is an extension of Pacelab APD, with system modelling added to it. It is necessary to take into account the systems of the aircraft when designing it, since they play an essential role in the energy requirements, overall mass, operating costs, fuel consumption and reliability. It includes a library with components that are part of the systems, divided into three categories: hydraulic, pneumatic and electrical. For most of the components, there is an explanation about its operation and input/output definition.

I.B.2. Boeing 737

In order to put into practice the results found in the previous research, both in the analysis of the aerodynamic impact and the modelling of the aircraft systems, a platform has been chosen to carry this out. The aircraft model used is the Boeing 737 Next Generation. This aircraft is the best-selling commercial jet aeroplane in history. It has been continuously manufactured by Boeing since 1967, with nearly 10,000 aircraft delivered and 4,489 orders yet to be fulfilled as of the end of 2017. For this reason, it is easier to find available open-source data about its systems and performance to carry out the analysis, and therefore it has been chosen. Its main characteristics are detailed in Table 1.

Table 1. Specifications of Boeing 737-600[1]

Length	35.8 m	Fuel capacity	26020 l
Wingspan	31.24 m	Powerplant	2 x 86.7 kN
Height	12.6 m	Cruise speed	0.785 Mach
Empty weight	36378 kg	Range	5436 km
Service ceiling	12500 m	MTOW	65544 kg

II. State of the Art of New powerplant Installations

According to the first objective of the study, an analysis is carried out to determine which are the aerodynamic impacts of the propulsive installation with respect to the aircraft. First, the aerodynamic impact of the traditional configuration is reviewed and those concepts will be then taken into consideration when introducing the new powerplant architecture, with a particular emphasis into the over-the-wing nacelle configurations. The most important conclusions drawn in the case of UWN configurations are that the main impact is caused by moving the nacelles along the longitudinal axis of the aircraft,[7–10] attaining the minimum drag when placing the nacelle furthest upstream from the wing.[8,10] The worst interference effects appear in the region between the inboard wing and the pylon.[11] The last conclusion extracted for this configuration[6] states that between the lower wing surface and the pylon the flow accelerates and a shock wave is created. At high speeds below Mach=1, the drag drops at high lift coefficients.[8]

II.A. Over-the-wing nacelle configurations

Depending on the place where the engines are installed, there will be advantages or disadvantages. When the engines are placed over the wing, the cabin size is maximised since the engine support structure is removed from the fuselage. If they are installed under the wing, there are issues such as ground clearance that have to be considered, especially in business jets and high by-pass-ratio engines. It has been traditionally thought that if they are installed over the wing, the drag interference increases, mainly at high speeds. Nevertheless, the empirical and simulation results carried out[12] express the opposite, as stated at the end of this section.

Over-the-wing nacelle configurations, such as in the Honda Business Jet, provide short take-off and landing, austere runway operations, water operations and a larger passenger cabin. This configuration also allows the mounting of high-bypass turbofans as well as community noise reduction since the wing shields the engine exhaust noise from ground observers. Besides, there are other advantages such as the avoidance of foreign-object damage, elimination of thrust gates for flaps, lighter and less constrained landing gear installations as well as increased crash worthiness for a collapsed-gear landing or a water ditching. Furthermore, all these advantages need not have trade-offs in centre-of-gravity placement and tail size of aft-fuselage nacelle installations. In particular, this configuration has been also chosen for this study because among the objectives of AEGIS, is considered the parameterisation of powerplant architectures, therefore the objective is to find the aerodynamic interactions between the engine nacelle and the airframe.

The method used in the three articles reviewed is the evaluation of the Euler equations.[13] The studies were made at Mach 0.73, with flow-through nacelles and lift coefficient of 0.4. In the second article studied from Hill[12] the nacelle has been mounted directly onto the wing with no pylon and the Mach number used was 0.78 with a lift coefficient of 0.44, taking the DLR-F6 aircraft. In the third article from Sasaki,[14] the analysis is made at Mach number 0.70, characteristic of the mid-sized, short-range aircraft, and the lift coefficient at 0.57.

Regarding the nacelle position with respect to the engine, the wave drag is minimised when the nacelle is placed at 80% of the chord, having found this result at a span location $Y/w = 0.72$ (Y: distance between the fuselage and the nacelle, w: width of the nacelle).[13] The drag is also minimised when $Z/h < 1$, (Z: distance between the wing and the nacelle, h: height of the nacelle). If this ratio is close to zero, a strong shock forms near the trailing edge of the wing, and if > 1, the wave-drag reduction would disappear.[13] In addition, the lower Z/h, the lower L/D. Therefore, as said before, Z/h must be less than one but not close to zero.[14] With respect to the aerodynamic performance of the wing and the nacelle, the best position of the nacelle is away from the wing, both higher and rearward. However, this would create both maintainability and structural problems. Therefore, the objectives are: maximising L/D while minimising Z/h and X/c.[14] In this article, the first optimisation was carried out on the wing and the nacelle, not the pylon, and the highest L/D configurations had both low $X/c=0.73$ and $Z/h=0.48$.

Considering the interferences, the fact of installing the nacelles over the wings has a strong influence on the aerodynamic performance because of the appearance of a shock wave between the wing and the nacelle, which increases the wave drag. Moreover, this fact has led to industry designs being overlooked.

A root fairing prevents a strong shock from forming at the root before the shock appears at the rest of the wing.[13] When the nacelle is located near the shock, it becomes weaker, the drag-divergence Mach number being even higher than for the clean configuration.[13] Regarding the pylon, the shock strength is smaller with it since the pylon reduces the velocity upstream.[13] The pitching-moment coefficient of the over-the-wing nacelle configuration is less negative than in the clean configuration, and therefore, reduced download of the horizontal tail is needed to trim the aircraft, resulting in lower trim drag.[13]

The inboard channel between the wing and the nacelle creates beneficial interference effects and it has to be optimised to produce maximum low-pressure lift with minimal shock-induced flow separation.[12] Its strength can be controlled through the position of the nacelle,[14] achieving this way better results than for the UWN configuration. At higher Mach than 0.78 and without considering viscosity, the drag rise of the OWN configuration is much milder, even attaining a lower drag coefficient than the wing-body (WB) configuration for Mach 0.82[12] (see Figure 1, left). However, taking the viscosity into account, and at high Mach number, the OWN configuration has a much lower transonic drag rise than the UWN one, although higher than the WB configuration[12] (see figure 1, right).

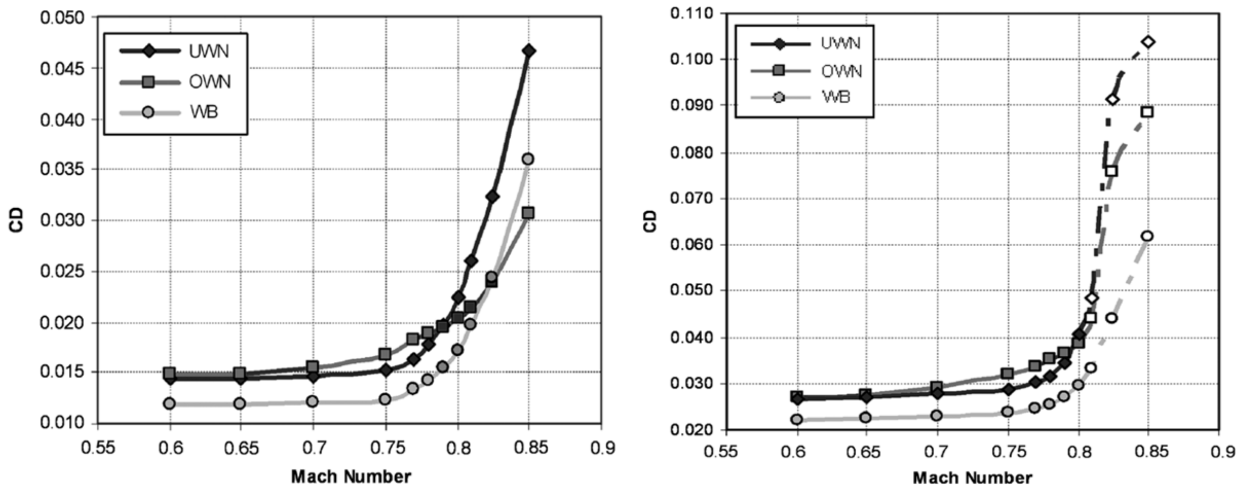

Figure 1. Euler drag-rise trends (left) and Navier-Stokes drag-rise trends (right)

III. Model implementation in *Pacelab APD*

Based on the litterature review accomplished, as previously explained, the objective is the introduction of changes into the structure of the software so as to be able to analyse more architectures than in the original version. It is desirable to introduce more aircraft configurations to take into account the possibilities studied beforehand. This way, the option to install the engines over the wings is created. In addition, one of the interests of this research is to find new aerodynamic models that are more accurate and consistent. Therefore, the way of modifying the existing models or adding new ones is explored and carried out in the *Pacelab Knowledge Designer* (KD) software.

For instance, a new function has been introduced that considers the drag interference coefficients between the nacelles and other components of the aircraft. It is based in the theory developed by the Roskam reference in its Chapter 5,[17] *ProfileDragCorrections_Chp12_5*.

Besides modifying the structure of the programme to allow the introduction of the new configuration, the aerodynamic model is enhanced by a more suitable interference model. This interference is originally taken into account through a coefficient,[16] whose value depends on how far the nacelles are installed from the wing or the fuselage. However, this coefficient was not actually considered when calculating the drag of the nacelles by the software, which could be observed since the change of its value did not have an impact on the drag coefficient of the nacelles. Therefore, besides introducing a detailed model more consistent, necessary modifications were implemented so that it is really taken into account.

For the drag interference coefficient, a parallel function was created.[17] First, the interference drag contribution due to the wing in the case of turboprop and piston-prop powerplants is calculated, eq. 4.63 of the *Roskam* reference.[17] Depending on the place where the engines are installed with respect to the airframe, the value of the interference factor is different. Then, the drag interference between the wing and the nacelles for jet-driven aircraft is found, eq. 4.64 of *Roskam* reference.[17] This figure depends on geometrical characteristics of the nacelle installation with respect to the wing as well as the Mach number. Besides, the interference drag which is caused by the interaction between the fuselage and the nacelle has been coded, eq. 4.65 of *Roskam* reference.[17] It depends on geometrical characteristics and on the lift coefficient. Moreover, the cooling drag coefficient increment has also been included, eq. 4.66, but which is only applicable for radial engines, this not being the case of the architectures under study. Finally, the drag interference increment that is due to windmilling conditions has been included, for the cases of jet engines and propellers, as well as the drag coefficient due to a stopped propeller, eqs. 4.67, 4.68 and 4.69 of *Roskam*[17] respectively.

The total drag coefficient of the aircraft is calculated. This is done by adding the contributions of the parts of the aircraft to it: wing, winglets, fin, stabiliser, canard, fuselage, nacelles and pylons. The function is modified so as to consider that the contribution of the nacelles is not only due to the nacelles themselves but also due to the interferences with the fuselage and the wing, as per Equation 1:

$$C_{D_{Nacelle}} = C_{D0_{Nacelles}}(1 + C_{Dint_{wing}}) + C_{Dint_{fus}}; \tag{1}$$

The function to calculate the isolated drag coefficient caused by a nacelle is taken from Roskam,[17] instead of Torenbeek[18] since it is considered to be more complete. The nacelle isolated drag coefficient is calculated by adding Equation 2, which is the drag coefficient created by the isolated nacelle, to Equation 3, which is associated to the drag created by the base of the nacelle, as per Equation 4.

With respect to the first objective of introducing a new architecture, the process is achieved, this is to say, following all the steps mentioned in Section 2.2.2 of the thesis report[4] on which this study is based, the desired configuration is added to the software.

$$C_{D0_{NacellesBase}} = R_{wf}\, C_{F_{fus}}\,(1 + \frac{60}{(\frac{l_f}{d_f})^3} + 0.0025\,\frac{l_f}{d_f})\,\frac{S_{wet}}{S} \tag{2}$$

R_{wf} is taken equal to 1, since the nacelle is considered to be alone in this calculation. $C_{F_{fus}}$ is the turbulent flat plate skin-fraction coeffient, found from Raymer.[16] l_f is the fuselage length, d_f is the maximum fuselage diameter, S_{wet} is the wetted surface of the nacelle, d_b is the fuselage base diameter and S_{fus} is the fuselage maximum frontal area.

$$C_{D_{bNacelles}} = 0.029\,\frac{(\frac{d_b}{d_f})^3}{\sqrt{C_{D0_{NacellesBase}}\frac{S}{S_{fus}}}}\,\frac{S_{fus}}{S} \tag{3}$$

$$C_{D0_{Nacelles}} = C_{D0_{NacellesBase}} + C_{D_{bNacelles}} \tag{4}$$

IV. Aircraft Systems in *Pacelab SysArc*

IV.A. Introduction to *Pacelab SysArc*

An aircraft is a complex collection of systems that has many different functionalities. Therefore, in order to accomplish all the requirements and needs for the successful development of the flight, many different systems have to be utilised. In order to understand how the systems are structured and how they work, the Flight Crew Operating Manual (FCOM),[5] has been used as a reference. The FCOM is issued as a guideline for operators to develop their own standard operating procedures, in accordance with applicable requirements. Nevertheless, in the scope of the study objectives, the attention will be centred on the analysis of the air conditioning system, the hydraulic system, the electrical system and the ice and rain protection system, in order to analyse how much non-propulsive energy is necessary to take from the engines.

Once the missing components and loads have been added in the Aircraft Systems structure, it is necessary to connect them, both logically and physically. This is carried out through pathways and routing. Pathways are the logical connection routes between the components. This is to say, they are not real, but represent the possible routes that will be assigned at a later stage. Once the pathways have been created, the routing process consists of defining the physical connections between the components. This way, ducts, pipes and wires are created.

IV.B. Environmental control system (ECS)

The objective of the air conditioning system is to provide the air so as to adapt the pressure and temperature of the different areas in which the cabin is divided: cockpit and passenger areas. In the model available in the software programme, one can observe that the system is duplicated so that in the case of failure, the function of the system can be always assured. For each of the two air conditioning packs, the first instance is the ram air inlet, which takes the air from the outside of the aircraft. Then, the air is split into two parts and compressed using an electrical compressor. This way, both the temperature and pressure of the air increase. Following this component, the air goes through an air cycle machine, which has the objective of providing the correct amount of air at the correct temperature and pressure to the cabin. Afterwards, the air is distributed to the different parts of the cabin using the mix manifold. In the series 3/5/6/700 of the aircraft, the temperatures of each of the zones are independently controlled,[15] while in 4/8/900 series the packs cool the coldest zone and the temperature of the others is regulated with trim air. The conditioned air enters the regulated compartments through the compartment inlet vents. Then, it goes out from the compartments through the compartment outlet vents, going back to the mix manifold. A representation of the modified model can be seen in Figure 2.

IV.C. Hydraulic system

The hydraulic system is used to provide power to actuate mainly the flight controls, landing gear and wheel brakes. The system is modelled with three reservoirs that contain the hydraulic fluid to be pressurised to actuate the systems. From each of the reservoirs, the fluid is transmitted to a pump, either mechanically or electrically driven. Then, it goes to a pressure module before entering a valve. From the 737-300 onwards, each hydraulic system had both an engine-driven pump (EDP) and an electric motor-driven pump (EMDP) to increase the redundancy.[15] Afterwards, depending on the component to power, the pressurised fluid is transmitted directly to the load or to actuators that power the components: ailerons, spoilers, elevators, slats, Krueger flaps and stand-by-rudder power control unit (PCU).

The precooler is part of the same heat exchanger that removes heat from the compressed air of the air cycle machine before it goes through the turbine. For this reason, it may be considered as part of the air cycle machine assembly. The water separator is a component through which the air passes that includes a polyester coalescer bag to collect the water. The air is forced to move circularly to condense the moisture before reaching the collection chamber where the water is separated from the air. The parameters represented in *SysArc* are the flow rate, pressure and temperature, but not the moisture content, which could be considered as a further development. Recirculation fans used for getting the air back to the mix manifold can be represented as electrical fans. For instance, 25% of the cabin air is recirculated for passenger comfort compared to 50% on the 757/767 and none on the MD80. The representation of the equipment cooling and the forward cargo compartment cooling is accomplished by adding more regulated compartments to the structure, paying attention to the fact that on the ground, it is an open circuit.

It is observed that the hydraulic system modelled by default in the software is not redundant since the standby system does not power the commands of systems A and B, this being necessary in case of failure so as to assure the correct operation of the flight control surfaces, for instance. In the real system, there are three hydraulic systems: A, B and standby. Moreover, the landing gear does not appear in this model, neither the wheel brakes, nose wheel steering, thrust reversers nor the autopilots. Pumps are lubricated and cooled by hydraulic fluid that returns to the reservoir via a heat exchanger. This not being represented in the model, since it would be necessary that the pumps had three inputs instead of two. The control of the rudder is not represented, performed by both the systems A and B. Components not represented have been added, mainly by using actuators, i.e. yaw dampers, normal and alternate brakes, wheel steering, landing gear and landing gear transfer unit, power transfer unit, thrust reversers, leading edge flaps and slats and standby yaw damper.

IV.D. Electrical system

The missing connections in the *SysArc* model for the electrical system network, are the supply from the battery to the APU starter, which cannot be represented in *SysArc* since the APU component has no inputs that are necessary to connect the battery. However, a DC bus has been added from the battery. In addition, the switch between the main battery and the auxiliary battery is added. In the existing model in *SysArc*, this system is not included, although it is necessary for the correct operation of the aircraft. For this reason, it has been implemented according to the specifications that can be found in the FCOM.

IV.E. Analysis of the losses

With the aim of having a closer approach to the real aircraft model, it exists the possibility of introducing losses. This means that we take into account the losses that are produced in electrical cables due to voltage drops and heat losses. Moreover, pressure losses in hydraulic pipes are also considered. Preliminary indications about the average voltage drops that occur in aircraft cables are found in the literature.[3] The voltage drop is set to 1% for the DC network (28 V) and 4% for the AC network (115 V).

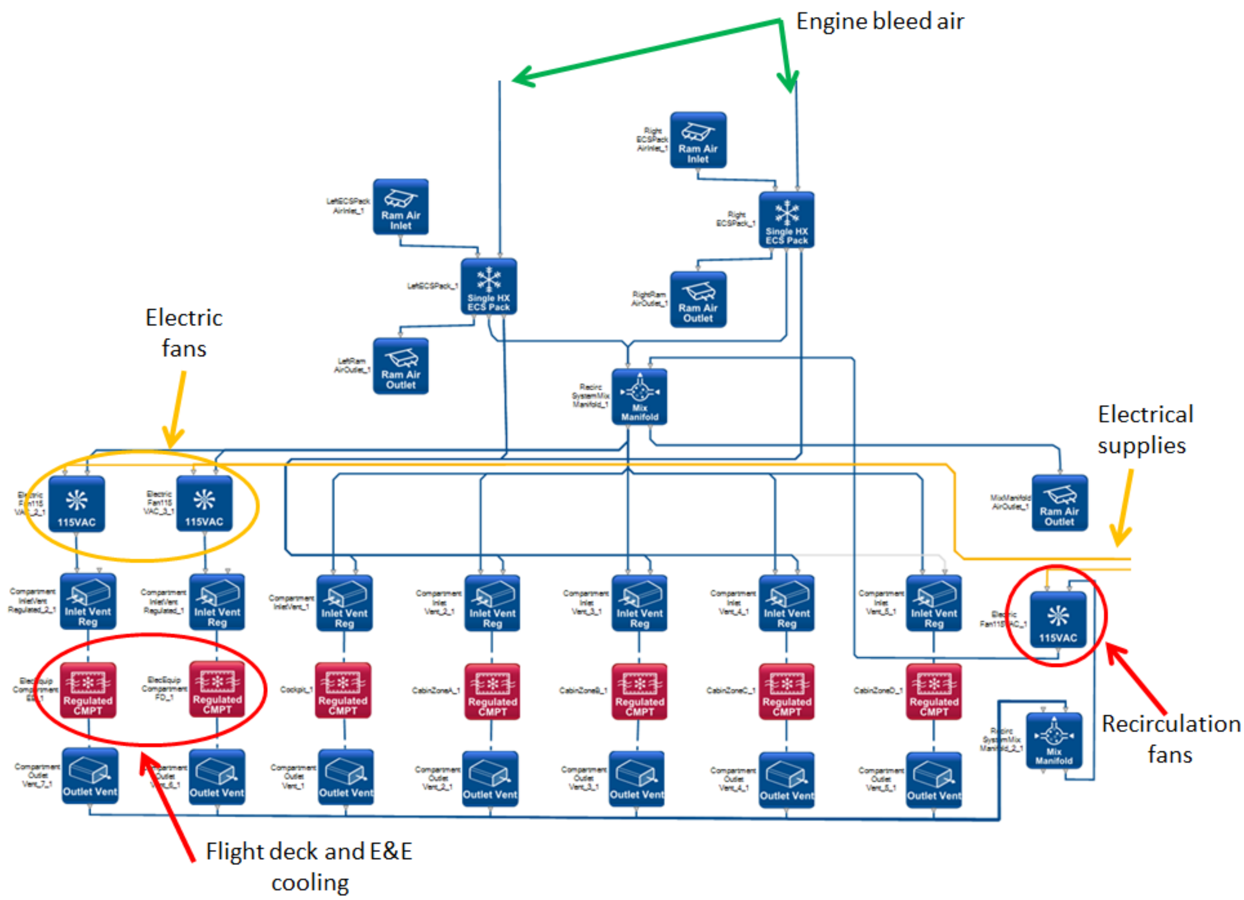

Figure 2. Modified air conditioning system arrangement

The generally used methods to calculate the pressure losses are mainly based on the Reynolds number and the pipe roughness. The following expression introduced by Darcy-Weisbach models this phenomenon, where L is the pipe length, ρ the density of the fluid, d the diameter of the pipe, v is the flow velocity and λ the friction factor which is related to the Reynolds number and the pipe roughness. ϵ is the pipe average roughness and d is the pipe inside diameter. According to the available data in *Pacelab SysArc*, the pipes are made of PVC, which has a roughness of between 0.0015 and 0.007 mm, taking for the calculations the value of 0.006 mm. Since d is 20 mm, for all the pipes, $\frac{\epsilon}{d}$ will be fixed at 0.0003.

$$\Delta p = \lambda \frac{L}{d} \rho \frac{v^2}{2}; \tag{5}$$

$$\lambda = \lambda \left(Re, \frac{\epsilon}{d} \right); \tag{6}$$

In order to determine λ, the Moody diagram is used for cylindrical pipes, which differentiates the fluid regime, whether it is laminar, turbulent or transitional. Furthermore, there are empirical expressions to determine λ that are largely used. For the cases in which Re $<$ 2000, the empirical expression 5 is used, while in the other cases this is calculated through the Moody diagram.

To fix the relative pressure drop that will be introduced to carry out the sizing, five hydraulic pipes are taken from the existing distribution elements in the *SysArc* model and an average is taken. The results are obtained having calculated the velocity, the Reynolds number and the friction coefficient. The pressure loss that is going to be introduced in the software is therefore calculated, obtaining a result of 0.0583 bar/m.

V. Energy Breakdown and Failure Modes

Up to this point, the system has already been built in *SysArc* since the missing components have been added, connected properly, the necessary compartments have been defined, the pathways and routing are performed and the loss considerations are introduced. Therefore, it is possible to carry out the energy breakdown analysis. First, the nominal case is analysed and then several failure modes: left engine failure, right engine failure, ice and rain protection system On and power transfer unit On. The objective is to assess how much energy has to be supplied by one single engine for non-propulsive purposes as well as the energy necessary when some systems are activated.

The first case for which results are obtained is the nominal case, in which the energy is obtained from the engines, the ice and rain protection system is Off as well as the power transfer unit and landing gear transfer unit. The engine model used is the CFM International CFM56-7B27 and the energy breakdown is chosen to be carried out at nominal conditions of altitude at 20000 ft, Mach number 0.6 and ISA standard day. Nearly 50% more shaft power is taken from the left engine than from the right one. Regarding the bleed air, which supplies the ECS system, the quantity is the same for both engines, therefore the difference in the shaft power is based on the electrical and hydraulic systems. Regarding the compartments, the heat load corresponds to the addition of the internal heat load, the external heat load and the heat transfer. The internal heat load is the addition of: the electrical, the hydraulic, the mechanical, the pneumatic, the sources and the miscellaneous and the occupants' heat loads.

Then, this previous nominal case is analysed but at standard cruise conditions. For this case, the energy is obtained from the engines, the ice and rain protection system is Off as well as the power transfer unit and landing gear transfer unit. The flight conditions are Mach at 0.785 while the altitude is 11000 m ISA standard day atmosphere. The total power rise with respect to the nominal case is 9.22%, being the left engine the one in which it becomes more pronounced. The total heat load rises four times and the total heat transfer does in a 77.9%. It is mainly in the cargo and cabin areas where the changes are the most pronounced. This is because the atmosphere conditions between the outside and the inside of the aircraft are more distinct at this altitude. A comparison between the two nominal cases is outlined in Table 5.

In the first failure mode, the left engine is thus set to the fail mode and the AC transfer bus 1, which is normally supplied by it, will be powered by the APU. The left engine supply is taken by the APU and the right engine continues to be available. In the case of the APU, the output nominal power is 50 kW, more than double the required power, while in the case of the right engine, the output nominal power is 250 kW. If the energy requirements of the AC transfer bus 1 were larger than 50 kW, there would be an exceedance and the APU would not be capable of supplying it.

The rise in the power in the AC transfer bus 1, see Table 2, comes from the EMDP pump of the hydraulic system A, which in the nominal case had a power demand of 2.092 kW, while in this case it is 4.162 kW. This is because the engine-driven pump is no longer available and the pressure production must be assumed by the EMD pump. It is found that the output energy supplied to the electrical components that depend on the left engine is three times the requirements of what is powered by the right engine.

Table 2. Output electric power comparison: nominal case .vs. left engine failure

2***AC transfer bus 1**	Left failure	18.46 kW
	Nominal case	16.39 kW
2***AC transfer bus 2**	Left failure	6.31 kW
	Nominal case	6.31 kW

Although the left ECS pack is inoperative, the compartments total heat load is the same, both in the nominal case and the left engine failure case. Nevertheless, this behaviour has an explanation: the ECS packs are responsible for the supply of trim air, which is the air directly bled from the compressor and therefore at a high temperature. The required quantity of trim air, however, is so small that when it is not supplied, the difference is not noticeable. Regarding the hydraulic system A, the pressure is supplied by the electrical motor driven pump, whose energy comes from AC transfer bus 1; because the engine-driven pump is not operative since it is supplied by the left engine.

In the case of the failure in the right engine, there is a noticeable difference in the output power of the AC transfer bus 2, as can be seen in table . The reason is mainly due to the power demand of the EMDP pump in the hydraulic system B, which in the nominal case needs an input power of 6.24 kW to work, while in the right engine failure case, this demand rises to 12.16 kW. In addition to that, the changes that take place for the left engine failure are applicable for this case as well.

Table 3. Output electric power comparison: nominal, left engine and right engine failures

3*AC transfer bus 1	Right failure	16.2 kW
	Left failure	18.46 kW
	Nominal case	16.39 kW
3*AC transfer bus 2	Right failure	12.18 kW
	Left failure	6.31 kW
	Nominal case	6.31 kW

The change in system performance due to the activation of the ice and rain protection system was then evaluated. This system is pneumatic and therefore works with air that is bled from the engines. The energy sources view of the energy breakdown will allow some changes with respect to the nominal case to be observed. There is an increase in the bleed mass flow that is taken from both engines, since half of the ice and rain protection system works with the left engine and the other half with the right engine.

The following step consists of powering on the transfer unit for the case when the electric motor-driven pump of the hydraulic system B fails. In this case the power transfer unit is activated to supply the required energy to the pressure module of the hydraulic system B. The shaft power from the left engine increases by 11.47 shp, while the shaft power from the right engine decreases by 9.3 shp. The EMDP of the hydraulic system B does not operate in this case and would be normally supplied by the right engine. The left engine will supply the power required by the power transfer unit. With respect to the electrical demand, the total quantity is very similar to that of the nominal case, since the energy which is not supplied to the hydraulic system B is compensated by energy supplied through system A, since the overall system works in the same conditions. The required pressure for the system B produced by the power transfer unit (PTU) is supplied by EDP A and EDMP A, which increase their power demand. A summary of the results is seen in Table 4.

Table 4. Pumps and AC transfer buses consumptions - nominal .vs. PTU On

	Nominal case [kW]	**PTU On [kW]**
AC transfer bus 1	16.23	21.33
AC transfer bus 2	6.311	0
EDP A	2.282	4.749
EDMP A	2.092	4.079
EDP B	6.829	7.429
EDMP B	6.242	Failure - not supplied
PTU	Off	2.831

Table 5. Summary of the changes between the two nominal cases

	Nominal (Mach 0.6)	**Nominal (Mach 0.785)**
Total energy source	49.91 shp	54.51 shp
Total bleed air	1.84 kg/s	1.6 kg/s
Total head load	-5.67 kW	-23 kW
Total heat transfer	-22.26 kW	-39.6 kW
Total electrical load	36.3 kW	40.89 kW

VI. Conclusions and Perspectives

After these analyses have been carried out, it is possible to highlight the work performed in comparison to the objectives and expectations set at the beginning, where two main global areas of research are proposed: the aerodynamic analysis of the powerplant installation and the study of the systems architecture.

A bibliographic study was necessary to perform so as to have a detailed insight of the potential new architectures to explore. Although not largely developed up to this day, these results unveil the high potential of over-the-wing nacelle configurations. The work is based on improving the existing software so that these findings are considered, first including new propulsion configurations and then the aerodynamic interferences. Therefore, the basis for the development of this configuration are set, due to the advantages that they present, not only in the aerodynamic terms of drag reduction, but also in the noise shielding that the fact of installing the engines over the wings creates, this being in compliance with the restrictions of airports in terms of noise impact.

With respect to the Boeing 737, an in depth analysis has been performed of the ECS, hydraulic, pneumatic and ice and rain protection systems, in order to understand how they work and how they are connected. It aimed to improve the existing model in *Pacelab SysArc*. This has been achieved above all by adding the missing components, as well as considering voltage and pressure losses.

The analysis of the energy breakdown of several working conditions carried out is a necessary step to assess how much energy is taken from the engines for purposes other than thrust power, as well as to analyse the impact of failure modes that may occur. Nonetheless, can be further completed, since for the moment the masses are set to zero by default and the location of the components is not exactly known as these manufacturer's data remain confidential.

In conclusion, this project has provided a deep understanding in the disposition and analysis of the aircraft systems. Most importantly, since it is a multidisciplinary project, it has provided a first step into several areas about how aircraft design may progress in the future to reach better performance, reduced consumption as well as innovative ways of evolving through new powerplant architectures.

References

[1]Boeing 737 description, http://www.boeing.es/productos-y-servicios/commercial-airplanes/737ng.page

[2]IATA, http://www.iata.org/pressroom/pr/Pages/2016-10-18-02.aspx

[3]Federal Aviation Administration, *Aircraft Electrical System*, Technical report, U.S. Department of Transportation, 2012.

[4]Rubio Cubas, Adrian, *Performance and Interactions Analysis of Powerplant on a SMR Civil Aircraft As a First Step Towards Innovative Integrated Propulsive Solutions*, DAEP, ISAE-SUPAERO, 2017.

[5]*Boeing 737 Flight Crew Operations Manual*, http://www.clubinformatiquedomont.fr/737-NG-FCOM-ISSUE-30.pdf

[6]Rossow, C.C. and Hoheisel, H., *Numerical Study of Interference Effects of Wing-Mounted Advanced Engine Concepts*, ICAS, 1994, vol 18.

[7]Rossow, C.C. and Godard, J.L. and Hoheisel, H. and Schmitt, V., *Investigations of Propulsion Integration Interference Effects on a Transport Aircraft Configuration*, Journal of Aircraft, Chesapeake, 1994, vol 31, no. 5, pp 1022-1030.

[8]Berry, D.L., *The Boeing 777 Engine/Aircraft Integration Aerodynamic Design Process*, ICAS, 1994, vol 94, chap. 6.4.4.

[9]Brodersen, O., *Drag Prediction of Engine Airframe Interference Effects Using Unstructured Navier Stokes Calculations*, Journal of Aircraft, 2002, vol 39, no. 6

[10]Benard, E. and Devine, R. and Cooper, R.K. and Gault, R. and Watterson, J.K., *Comparison of Conventional and Compression Pylon Designs for an Underwing Nacelle*, Journal of Aircraft, 2009, vol 46, no. 1

[11]Ingraldi, A.M. and Kariya, T.T. and Re, R.J. and Pendergraft, O.C., *Interference Effects of Very High-Bypass Ratio Nacelle Installations on a Low-Wing Transport*, ASME, 1991, vol 114, no. 4

[12]Hill, G.A. and Kandil, O.A., *Wave-Drag Characteristics of an Over-the-Wing Nacelle Business-Jet Configuration*, Journal of Aircraft, 2009, vol 46, no. 1, pp. 25-35

[13]Fujino, M. and Kamawara, Y., *Aerodynamic Investigations of an Advanced Over-the-Wing Nacelle Transport Aircraft Configuration*, Journal of Aircraft, 2003, vol 40, no. 6, pp. 1177-1184

[14]Sasaki, D. and Nakahashi, K., *Aerodynamic Optimization of an Over-the-Wing-Nacelle-Mount Configuration*, Journal Modelling and Simulation in Engineering, 2011

[15]Brady, C., *The Boeing 737 Technical Guide*, Tech Pilot Services Ltd, 2017

[16]Raymer, D.P., *Aircraft Design: A Conceptual Approach*, AAIA Educational Series, 1992

[17]Roskam, J., *Roskam Aviation and Engineering Corporation*, Roskam Aviation and Engineering Corporation, 1987

[18]Torenbeek, E., *Synthesis of Subsonic Airplane Design*, Kluwer Academic Publishers, 1982